Analysis of nuclear-quadrupole-resonance spectrum of incommensurate phases: The case of bis(4-chlorophenyl) sulfone

J. Schneider, C. Schürrer, A. Wolfenson, and A. Brunetti
FaMAF, Universidad Nacional de Córdoba, Medina Allende y Haya de la Torre, Ciudad Universitaria, 5000 Córdoba, Argentina
(Received 30 December 1996; revised manuscript received 3 October 1997)

In this work, previous experimental studies of the ^{35}Cl nuclear-quadrupole-resonance (NQR) line shape in the incommensurate phase of bis(4-chlorophenyl) sulfone were extended. The broad spectra in the incommensurate phase (IC) were measured using the Fourier transform of the nuclear signal to avoid systematic errors committed in some studies of this compound. The results were interpreted within the framework of the general treatment developed by Perez-Mato, Walisch, and Petersson. The effects of the incommensurate modulation on the asymmetry parameter of the electric-field gradient were explicitly included in the expression of the NQR frequency. The features of the spectra were adequately reproduced in the whole temperature range, by considering the nonsinusoidal character of the atomic modulations reported by x-ray diffraction. No evidences were found concerning IC wave fluctuations smearing out the singularities of the NQR spectrum. On the other hand, relative intensity of NQR peaks and temperature behavior of some parameters of the plane-wave ''local'' model were explicitly calculated. Comparison of these quantities with the experimental results excludes the applicability of the ''local'' model in the case of bis(4-chlorophenyl) sulfone. [S0163-1829(98)06006-8]

I. INTRODUCTION

The nuclear-quadrupolar-resonance (NQR) technique has been used for several years in the study of structural and dynamical properties of incommensurate (IC) phases.[1] The inhomogeneous broadening of the NQR line shape in the IC phase depends basically on two different factors. The first one is the relation between the NQR frequency at a nuclear site and the atomic displacements of its neighbors produced by the IC modulation. This factor expresses merely how the structural distortions are translated by the local physical observable of the NQR experiments. The second and more interesting factor is the particular spatial dependence of the atomic modulation functions, intrinsic to the structure of the IC system under study.

The bis(4-chlorophenyl) sulfone (BCPS) presents an IC phase below $T_I = 150$ K, widely studied by different experimental techniques, including NQR of ^{35}Cl nuclei.[2–6] The ^{35}Cl NQR studies have shown some discrepancies about the observed line shape in the IC phase. Nevertheless, the spectral densities reported in Refs. 3, 5, and 6 can be affected by strong distortions due to an inadequate experimental method, as will be discussed in Sec. III. Most of the subsequent analysis of the IC phase carried out by these authors is mainly supported on the measured line shapes. So, it becomes important to obtain more reliable experimental data in order to check the validity of some proposed features of the IC phase of BCPS, like fluctuations of the IC wave at temperatures down to 10 K below T_I.[6]

On the other hand, the analysis of the NQR spectra of BCPS performed in all previous works[2–6] lies on the so-called ''local'' model or its improved version, the nonlocal model.[7,8] In these works, the IC modulation was assumed as a plane wave down to 80 K, approximately. Nevertheless, x-ray-diffraction measurements yielded direct experimental evidence of nonsinusoidal atomic modulation functions at 90 K,[9] as it was previously suggested by elastic neutron scattering[10] at temperatures lower than 100 K.

In order to consider these experimental information, a more general approach, developed by Perez-Mato, Walisch, and Petersson,[11] can be used to analyze the observed NQR spectrum. Within this formalism no particular assumptions are made, either on the spatial dependence of the modulation functions or on the relation between the electric-field-gradient (EFG) tensor elements and nuclear displacements. Also, the parameters involved by the model in the description of the NQR spectrum can be readily correlated with experimental structural information.

In this work, a previous experimental study of the NQR line shape in the IC phase of BCPS (Ref. 4) was extended. The whole ^{35}Cl NQR spectrum was reconstructed in the IC phase as a function of temperature between 80 and 150 K. The inhomogeneously broadened spectrum was obtained by means of Fourier transform of the NQR echo signals. As discussed in Sec. III A, this experimental procedure is appropriate when the line shape exhibits sharp peaks. A general analysis of the temperature behavior of some parameters of the ''local'' model and the relative intensity of the NQR peaks was performed in Sec. II A. These quantities were compared with the experimental results, in order to test the applicability of the ''local'' model to the case of BCPS. The analysis of the experimental data were carried out according to the formalism of Perez-Mato *et al.*, briefly reviewed in Sec. II B. Also, in Sec. II C, the effects of the IC modulation on the asymmetry parameter of the EFG at chlorine sites were explicitly considered. The new experimental data and its discussion are presented in Sec. IV.

II. THEORY

A. NQR spectrum of IC phases: The ''local'' model

As was mentioned above, the results of previous NQR studies of BCPS were interpreted in the frame of the ''local'' model.[1] In this section, the main features of the spectrum

predicted by this model are summarized, including some calculations about the frequency position and intensities of the NQR peaks. These results provide a tool to test the applicability of the quadratic ''local'' model in a particular case, by rapid inspection of the relative intensities of the NQR peaks.

In the ''local'' model, the NQR frequency ν^{μ} of a given nucleus with coordinate x is expanded only in powers of the displacement u of the nucleus itself and the displacements *in phase* of all nuclei interacting with it. When the IC modulation is one dimensional and all the relevant displacements are described by plane waves $u=\cos(\varphi(x)+\varphi_0)$, it can be written:[1,10]

$$\nu^{\mu}=\nu_0+\nu_1\cos(\varphi(x)+\varphi_0)+\frac{\nu_2}{2}\cos^2(\varphi(x)+\varphi_0)+\cdots, \tag{1}$$

where $\varphi(x)=kx$, k being the incommensurate wave vector. The coefficients ν_n are proportional to the nth power of the amplitude of the frozen modulation wave A, which is the order parameter of the normal-IC phase transition with critical exponent β:[1]

$$\nu_n\propto A^n\propto(T_I-T)^{n\beta} \quad n=1,2,\ldots. \tag{2}$$

In the whole crystal, $\cos(\varphi)$ takes quasicontinously all values between -1 and 1. Thus, reducing the phase φ to the interval $[0,2\pi)$, the spectral density at a given frequency ν can be obtained as[1]

$$F(\nu)\propto\sum_{\varphi_i}\frac{1}{2\pi|d\nu/d\varphi|_{\varphi_i}}, \tag{3}$$

where the summation runs over all phase values φ_i satisfying in Eq. (1) $\nu^{\mu}(\varphi_i(x))=\nu$. The NQR spectrum $L(\nu)$ is obtained by means of the convolution of $F(\nu)$ with the homogeneous line shape $h(\nu)$. The peaks observed in $L(\nu)$ are related to singularities of the inhomogeneous spectral density $F(\nu)$. If only the linear and quadratic terms are kept in expansion (1), as some authors have considered for BCPS,[3,5] and the relationship $|\nu_2|>|\nu_1|$ holds, there will be three singularities at frequencies[1]

$$\nu_A=\nu_0+\nu_1+\frac{\nu_2}{2};\quad \nu_B=\nu_0-\nu_1+\frac{\nu_2}{2};\quad \nu_C=\nu_0-\frac{\nu_1^2}{2\nu_2}. \tag{4}$$

From expression (2), it must be noted that the frequency ν_C is independent of the order parameter, so the difference $\nu_C-\nu_0$ is independent of temperature. On the other hand, if the case $|\nu_2|\leqslant|\nu_1|$ holds, only the singularities at ν_A and ν_B are present. In order to check experimentally these results, it is necessary to obtain the temperature behavior of the coefficients ν_0, ν_1, and ν_2. This can be done by inverting relationships (4), yielding

$$\nu_0=\frac{\nu_A+\nu_B}{4}+\frac{\nu_C}{2}\pm\frac{1}{2}\sqrt{(\nu_A-\nu_C)(\nu_B-\nu_C)}, \tag{5a}$$

$$\nu_1=\frac{\nu_A-\nu_B}{2}, \tag{5b}$$

$$\nu_2=\nu_A+\nu_B-2\nu_0. \tag{5c}$$

As can be seen from the square root in Eq. (5a), the frequency of the singularity at ν_C must be greater or lower than the others.

On the other hand, it is possible to calculate the relative intensity of the peaks in the NQR spectrum, located at the frequencies given in Eq. (4). The intensities can be compared among themselves by studying the behavior of $F(\nu)$ near the singularities. The summation in the general expression (3) arises from the fact that the relation between phase and frequency is multivaluated, as can be seen from Eq. (1). In order to simplify the expression of $F(\nu)$, it is convenient to define the quantities $r\equiv\nu_2/\nu_1$ and $X\equiv(\nu-\nu_0)/\nu_1$. Then, regarding only first- and second-order terms in Eq. (1), the derivative of $\nu(\varphi)$ satisfies

$$\frac{d\nu}{d\varphi}\propto\frac{dX}{d\varphi}=\sin(\varphi)[1+r\cos(\varphi)].$$

A new variable can be defined as $Y=1+r\cos(\varphi)$ within the range $[1-|r|,1+|r|]$. In this way, the spectral density can be expressed as a unique term $F(Y)$ in all the domain of Y:

$$F(Y)=\frac{1}{|Y|\sqrt{1-[(Y-1)/r]^2}}.$$

The positions of the singularities are $Y_A=1+r$, $Y_B=1-r$ and $Y_C=0$. As can be seen, the singularities Y_A and Y_B are located at the edges of the distribution $F(Y)$. The third singularity at Y_C exists only if $|r|\geqslant1$, collapsing with Y_B when the equality holds.

The relationship between Y and X is $Y=\pm\sqrt{1+2rX}$. Figure 1 shows the plot of $Y(X)$ for positive and negative values of r. As can be seen in the figures, the values X_A, X_B, and X_C, associated with the singularities at Y_A, Y_B, and Y_C, satisfy two possible order relationships depending on the sign of r:

$$X_C\leqslant X_B<X_A \quad r\geqslant1 \tag{6a}$$

or

$$X_B<X_A\leqslant X_C \quad r\leqslant-1. \tag{6b}$$

These inequalities among the positions of the singularities can be readily expressed in terms of frequencies by using the definitions of r and X:

$$\nu_C\leqslant\nu_B<\nu_A \quad r\geqslant1 \tag{7a}$$

or

$$\nu_B<\nu_A\leqslant\nu_C \quad r\leqslant-1. \tag{7b}$$

Now, the comparison of intensities of peaks in the NQR spectrum can be readily obtained by considering $F(Y)$. It is necessary to take the limiting value of the ratio of spectral intensities $F(Y)$ in the neighborhood of the singularities. The cases of positive and negative r can be considered.

Case $r\geqslant1$: The ratio between the edge singularities in the Y domain is

$$\frac{I(Y_A)}{I(Y_B)}=\lim_{\varepsilon\to0^+}\frac{F(Y_A-\varepsilon)}{F(Y_B+\varepsilon)}=\left|\frac{1-r}{1+r}\right|\leqslant1,$$

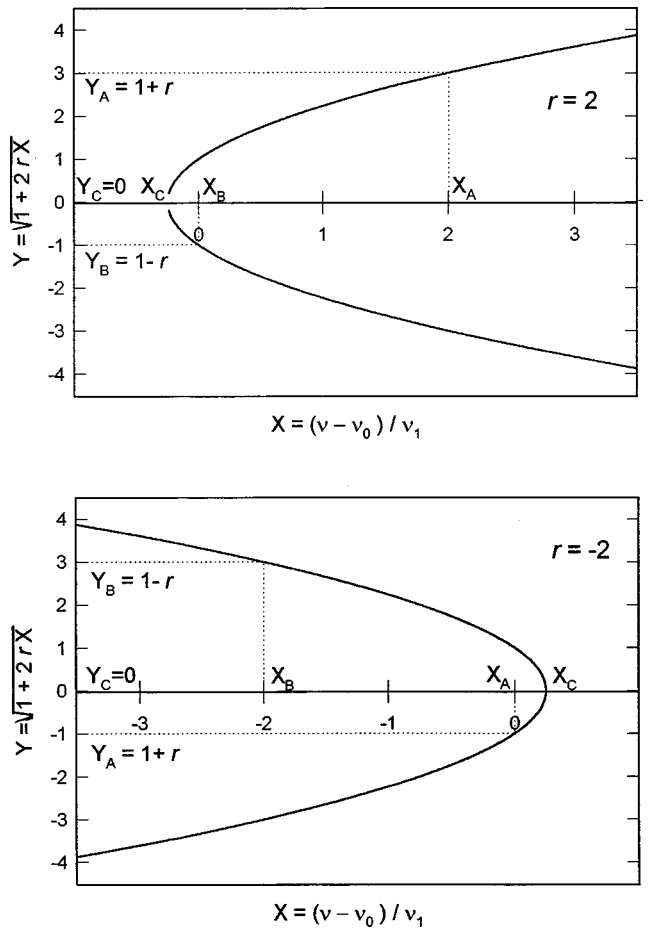

FIG. 1. Plots of the relation between the variables Y and X for $r=2$ and $r=-2$.

and with respect to the third singularity

$$\frac{I(Y_B)}{I(Y_C)}=\lim_{\varepsilon\to 0^+}\frac{F(Y_B+\varepsilon)}{F(Y_C+\varepsilon)}=0.$$

This two results leads to the inequality $I(Y_A)\leqslant I(Y_B)<I(Y_C)$, which can be more conveniently expressed in terms of frequencies, taking into account the relationships (6a) and (7a):

$$I(\nu_{\text{High Frec}})\leqslant I(\nu_{\text{Central Frec}})<I(\nu_{\text{Low Frec}}). \tag{8}$$

Case $r\leqslant -1$: In a similar way, the ratios between singularities can be obtained as

$$\frac{I(Y_A)}{I(Y_B)}=\lim_{\varepsilon\to 0^+}\frac{F(Y_A+\varepsilon)}{F(Y_B-\varepsilon)}=\left|\frac{1-r}{1+r}\right|\geqslant 1$$

and

$$\frac{I(Y_A)}{I(Y_C)}=\lim_{\varepsilon\to 0^+}\frac{F(Y_A+\varepsilon)}{F(Y_C+\varepsilon)}=0$$

yielding in this case $I(Y_B)\leqslant I(Y_A)<I(Y_C)$, which can be expressed in terms of frequencies, using Eqs. (6b) and (7b)

$$I(\nu_{\text{Low Frec}})\leqslant I(\nu_{\text{Central Frec}})<I(\nu_{\text{High Frec}}). \tag{9}$$

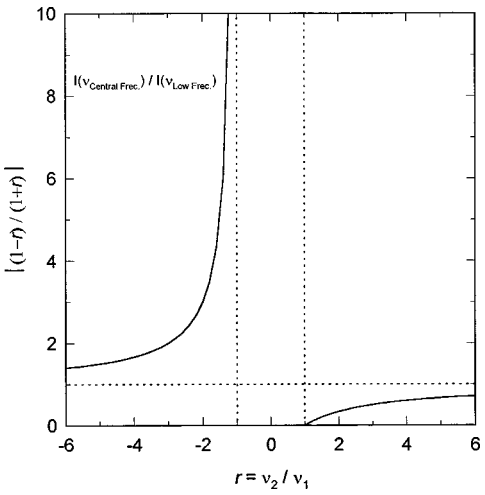

FIG. 2. Dependence of quantity $|(1-r)/(1+r)|$, which gives the intensity $I(\nu_{\text{High Frec}})/I(\nu_{\text{Central Frec}})$ for $r>1$ and $I(\nu_{\text{Central Frec}})/I(\nu_{\text{Low Frec}})$ for $r<-1$.

Therefore, the ''local'' model with a quadratic relation between ν^{μ} and u, predicts through expressions (8) and (9) that NQR peaks appear always with descending or ascending heights in the sense of ascending frequencies. The most intense peak is associated with ν_C and is located at one of the edges of the spectrum.

Figure 2 shows the dependence of the factor $|(1-r)/(1+r)|$, which is the ratio $I(\nu_{\text{High Frec}})/I(\nu_{\text{Central Frec}})$ for $r>1$ and the ratio $I(\nu_{\text{Central Frec}})/I(\nu_{\text{Low Frec}})$ for $r<-1$. As can be seen from the plot, the asymptotic behavior associated with a strong quadratic dependence implies the same intensities of the peaks at ν_A and ν_B.

B. General expansion of the EFG

In spite of the extensive use of the plane-wave ''local'' model to explain the NQR measurements in BCPS,[2–6] there are some basic hypothesis not satisfied in the case of this compound.

In molecular crystals, the interaction between the nuclear quadrupole of a given specie and the EFG is essentially a ''local'' phenomenon. The EFG at the nuclear site is determined by the surrounding electronic cloud, which depends basically on the bounded neighbors. So, in the IC phase of BCPS, the distorted EFG at the chlorine nucleus will depend not only on the Cl displacement, but on C and H displacements too. The relative phase of the modulation of one of these atoms with respect to the Cl atom *will not* generally be zero.

On the other hand, in a careful structural analysis of the IC phase of BCPS (Ref. 9) performed by means of x-ray diffraction, there was clearly demonstrated the nonsinusoidal character of the atomic modulations at 90 K. The displacement function of Cl atoms is composed by the first and second harmonics of the wave vector $\mathbf{q}=0.780\,\mathbf{b}^*$, with a nonzero relative phase between them. Furthermore, this modulation is not in phase with the displacements of C and H neighbor atoms.[9]

Therefore, in order to analyze the NQR data of BCPS, it is necessary to use a more general expansion of ν^{μ} in terms of the atomic displacements of the neighbors. The model

must consider vectorial character of the atomic displacements, nonsinusoidal behaviors, and mutual dephasing among modulations of different atoms. This treatment was already developed in a very general way by Perez-Mato, Walisch, and Petersson,[11] including the ''local'' and nonlocal approaches as particular cases.

The atomic displacements in the IC phase are expanded in a generalized Fourier series.[11]

$$\mathbf{u}(\mu,\mathbf{T})=\sum_{n=0,\pm1,\pm2\ldots}\mathbf{u}_n^{\mu}e^{in\mathbf{k}\cdot\mathbf{T}}, \tag{10}$$

where $\mathbf{T}$ identifies a cell of the crystal, μ is some kind of atom inside this cell ($\mu=1,\ldots,s$), and $\mathbf{k}$ is the incommensurate wave vector. The amplitudes $\mathbf{u}_n^{\mu}$ are complex vectors varying for each kind of atom μ. Also, the amplitudes and phases of each component can be different for a given μ. The EFG tensor at the nuclear site μ can be expressed in terms of all displacements as[11]

$$\underline{V}(\mu,\mathbf{T})=\underline{V_N^{\mu}}+\sum_{\alpha,\mathbf{T}'}\Phi_1^{\mu}\left(\begin{smallmatrix}\alpha\\ \mathbf{T}'-\mathbf{T}\end{smallmatrix}\right)\mathbf{u}(\alpha,\mathbf{T}')+\frac{1}{2}\sum_{\alpha,\beta}\sum_{\mathbf{T}',\mathbf{T}''}\mathbf{u}(\alpha,\mathbf{T}')\Phi_2^{\mu}\left(\begin{smallmatrix}\alpha\\ \mathbf{T}'-\mathbf{T}\end{smallmatrix},\begin{smallmatrix}\beta\\ \mathbf{T}''-\mathbf{T}\end{smallmatrix}\right)\mathbf{u}(\beta,\mathbf{T}'')+\cdots. \tag{11}$$

By using Eq. (10) in Eq. (11), a Fourier series expansion can be written for the EFG:[11]

$$\underline{V}(\mu,\mathbf{T})=\underline{V_N^{\mu}}+\sum_{n=0,\pm1,\pm2\ldots}\underline{V_n^{\mu}}e^{in\mathbf{k}\cdot\mathbf{T}}, \tag{12}$$

where each Fourier amplitude depends, in principle, on all the Fourier amplitudes of the atomic displacements (10) and all Taylor coefficients in Eq. (11). An element of the EFG tensor can be written as[11]

$$V_{ij}^{\mu}(v)=V_{Nij}^{\mu}+V_{0ij}^{\mu}+2\sum_{n>0}|V_{nij}^{\mu}|\cos(nv+\Psi_{nij}^{\mu}), \tag{13}$$

where the continuous internal coordinate $v\equiv\mathbf{k}\cdot\mathbf{T}$ has been used instead of the discrete variable $\mathbf{T}$.[11] The quantities Ψ_{nij}^{μ} are the phases of the complex Fourier amplitudes in Eq. (10).

A rough approximation of expression (11) for the Cl atoms on BCPS, can be performed assuming the following conditions:

(i) the relation among the EFG components and the atomic displacements is linear,

(ii) the relevant atomic displacements in Eq. (11) are the displacements corresponding to the Cl atom and the only bounded C atom.

So, from Eq. (11) the components of the EFG tensor at the Cl sites can be written as

$$V_{ij}^{\mathrm{Cl}}(v)=V_{Nij}^{\mathrm{Cl}}+V_{0ij}^{\mathrm{Cl}}+\Phi_{1ij}^{\mathrm{Cl}}(\mathrm{Cl})\mathbf{u}_{\mathrm{Cl}}(v)+\Phi_{1ij}^{\mathrm{Cl}}(C)\mathbf{u}_{\mathrm{C}}(v), \tag{14}$$

where the atomic modulation functions for Cl and C_4 are known from the x-ray study[9]

$$\mathbf{u}_{\mathrm{Cl}}(v)=\sum_{i=x,y,z}[A_i\cos(v+\alpha_i)+B_i\cos(2v+\beta_i)],$$

$$\mathbf{u}_{\mathrm{C}}(v)=\sum_{i=x,y,z}[C_i\cos(v+\gamma_i)+D_i\cos(2v+\delta_i)].$$

Then, expression (12) can be rewritten by grouping the oscillating terms with periodicity 1 and 2:

$$V_{ij}^{\mathrm{Cl}}(v)=V_{Nij}^{\mathrm{Cl}}+V_{0ij}^{\mathrm{Cl}}+Q_{ij}\cos(v+\Omega_{1ij})+P_{ij}\cos(2v+\Omega_{2ij}). \tag{15}$$

In this simplified approach, only harmonics up to second order are present in the modulation of the EFG components.

C. Pure NQR frequency in the IC phase

In pure NQR of nuclei with spin $I=3/2$, the resonance frequency is

$$\nu=CV_{zz}\sqrt{1+\eta^2/3}, \tag{16}$$

where z is the direction of maximum EFG, η is the asymmetry parameter defined as

$$\eta=\frac{V_{xx}^{\mu}-V_{yy}^{\mu}}{V_{zz}^{\mu}},$$

and $C=eQ/2\eta$, eQ being the quadrupolar moment of the nucleus. In the simple case of an axially symmetric EFG, $\eta=0$, and the resonance frequency results are proportional to V_{zz}^{μ}. If expression (13) is used, the NQR frequency can be written in general way as

$$\nu^{\mu}(v)=\nu_N^{\mu}+\nu_0+2\sum_{n>0}\nu_n\cos(nv+\Psi_n). \tag{17}$$

Although expressions (1) and (17) are formally similar, they are basically different, as was carefully pointed out by Perez-Mato, Walisch, and Petersson.[11] Analyzing the meaning of higher harmonics in those expressions, it can be shown that in Eq. (1) they are due purely to nonlinear effects in the relationship between ν and the displacements. On the other hand, in expression (17) higher harmonics in the modulation of the EFG can appear even with a first-order approach in Eq. (11). So, within the linear approximation (14) the resulting NQR frequency for the axially symmetric case is

$$\nu(v)=\nu_N+\nu_0+2\nu_1\cos(v)+2\nu_2\cos(2v+\alpha), \tag{18}$$

where the indexes indicating the Cl atom of BCPS were dropped. The higher harmonics in $\nu(v)$ arise purely from the intrinsic behavior of nuclear displacements.

The same considerations discussed above are still valid if the improved version of the nonlocal model is considered.[7,6] In this case, phase difference among nuclear displacements is regarded, but all the distortions are assumed as single-harmonic functions of $\varphi(x)$.

On the other hand, the possible distortion of the EFG symmetry by the IC modulation is not considered explicitly in usual treatments. The axial symmetry of the normal phase EFG can be locally lost in the IC phase due to, for example, distortions in the bond angles of the nuclei. In expres-

sion (16), variations of 0.02 in η gives an increase of 0.01% of the NQR frequency. Those values are well above the resolution of the usual NQR measurements. So in BCPS, where the Cl-C_4-C_3 bond angle can range between 119.2° up to 120.1°,[9] the perturbation produced by the modulation on the asymmetry parameter could be non-negligible.

Assuming that the value of η does not exceed 0.1, as it is observed in a variety of chlorinated benzene derivatives, expression (16) can be approximated as

$$\nu = CV_{zz}\left(1+\frac{\eta^2}{6}\right).$$

The asymmetry parameter η can be expanded in terms of the EFG components. Using the Laplace equation $V_{xx}+V_{yy}+V_{zz}=0$ for the electric field results in

$$\nu = C\left(\frac{7}{6}V_{zz}+\frac{2}{3}V_{xx}+\frac{2}{3}\frac{(V_{xx})^2}{V_{zz}}\right).$$

An additional simplification can be made neglecting the modulation effects on the term $1/V_{zz}$, resulting in

$$\nu = C\left(\frac{7}{6}V_{zz}+\frac{2}{3}V_{xx}+\frac{2}{3}\frac{(V_{xx})^2}{V_{Nzz}}\right). \tag{19}$$

This expression for the NQR frequency takes into account the modulation on the principal value V_{zz} of the EFG and on the asymmetry parameter η. If the simplified expression (15) for the V_{ii} is considered, then the two first terms in Eq. (19) gives modulations at frequencies 1 and 2, as in Eq. (18). The term with $(V_{xx})^2$ introduces harmonics of order 2, 3, and 4.

In any case, the NQR line shape can be obtained from the normalized frequency distribution, if the modulation function of the NQR frequency $\nu(\upsilon)$ is known:[11]

$$F(\nu)\propto\frac{1}{2\pi}\sum_{\upsilon'}\frac{1}{|[d\nu(\upsilon)/d\upsilon]_{\upsilon=\upsilon'}|}. \tag{20}$$

For a given ν, the sum goes over all values υ' satisfying $\nu^{\mu}(\upsilon')=\nu$ inside the interval $[0,2\pi)$.

III. EXPERIMENTAL

A. Measurement of broad inhomogeneous NQR line shapes

In order to determine the spectral density $F(\omega)$, two alternative experimental approaches can be followed. The first of them was established in Refs. 12,13 and consists of recording the maximum intensity of the echo signal $S_I(t=0;\omega_0)$ after a $\pi/2$-τ-π pulse sequence, as a function of the irradiation frequency ω_0 (the time origin is set at a time τ after the π pulse). Under certain conditions, as will be discussed below, the profile of the obtained function $S_I(0;\omega)$ is directly related to the shape of $F(\omega)$. The other approach involves the recording of the intensities $I(\omega_0)$ of the Fourier transform of the right half side of the echo signal $S_I(t;\omega)$, as a function of the irradiating frequency ω_0.

Regarding the first procedure, some care must be taken in a particular NQR experiment to check the validity of the basic hypothesis

$$S_I(0;\omega_0)=cte\cdot F(\omega_0). \tag{21}$$

Strictly, the relation between the intensity of the NQR echo signal and the spectral density $F(\omega)$ is

$$S_I(0;\omega_0)=\beta H(0)\int_0^{\infty}F(\omega)G(\omega_0-\omega)d\omega, \tag{22}$$

where ω_0 is the irradiation frequency, $H(0)$ is the Fourier transform of the homogeneous line shape $h(\omega)$, evaluated at $t=0$, and $G(\omega)$ is a function related to the response of the rf pulse, defined according to Katowski and Mackowiak.[14] The quantity $\beta<1$ depends on the characteristic decay time of the echo amplitude. Expression (22) was demonstrated by Pratt[15] for the particular case of a $\pi/2)_0$-τ-$\pi/2)_{90}$ sequence, and can be readily extended for the $\pi/2$-τ-π sequence using the ideas of Su and Armstrong.[16] As can be seen from Eq. (22), in general $S_I(0;\omega_0)$ *is not* directly proportional to $F(\omega_0)$, but it is an average of $F(\omega)$ with the response function $G(\omega)$. Relationship (21) holds only when $F''(\omega)\cong 0$ for all values of ω inside the interval $|\omega-\omega_0|>1/t_w$, where $G(\omega-\omega_0)$ assumes non-negligible values. For t_w on the order of tenths of μs, the interval of convolution is of tenths of KHz.

On the other hand, the method of measurement of $F(\omega)$ involving Fourier transform of the echoes is well-established in nuclear magnetic resonance,[17] and its validity can be extended to NQR. The intensity of $I(\omega)$, the Fourier transform of $S_I(t;\omega)$, evaluated at the irradiation frequency ω_0 is

$$I(\omega_0)=\beta\int_0^{\infty}F(\omega')h(\omega_0-\omega')G(\omega_0-\omega')d\omega'. \tag{23}$$

Due to the homogeneous line shape $h(\omega)$ assumes non-negligible values within an interval $\delta\leqslant 1$ KHz around ω_0, the width of the weight function $h(\omega)G(\omega_0-\omega)$ is two orders of magnitude less than the width of $G(\omega)$. In this situation, it is valid to expand $F(\omega)$ and $G(\omega)$ up to second order around ω_0 in Eq. (23), resulting in

$$I(\omega_0)=\beta F(\omega_0)\left\{1+\frac{M_2}{2}\left(G''(\omega_0)+\frac{F''(\omega_0)}{F(\omega_0)}\right)\right\}, \tag{24}$$

where M_2 is the second moment of the homogeneous line. The quantity β is usually independent of ω in the whole spectrum. So, expression (24) shows that $I(\omega_0)$ is proportional to $F(\omega_0)$. By explicit evaluation of the derivatives of $G(\omega)$, it can be shown that $M_2G''(\omega_0)$ is of the order of $M_2/\omega_1^2\cong 10^{-3}$, so this term can be neglected. The term $M_2F''(\omega_0)/F(\omega_0)$ depends on the particular shape of the spectral density. In order to estimate maximum values that can be assumed by this term, it can be evaluated near a peak and a singularity of the kind $(\omega-\omega_s)^{-\alpha}$ (with $\alpha<1$). In the former case, this term is less than $(\delta/\sigma)^2$ where σ is the characteristic width of the peak, while in the latter is $[\delta/(\omega-\omega_s)]^2$. In both cases $M_2F''(\omega_0)/F(\omega_0)$ can be neglected if

$$\sigma^2\gg\delta^2, \tag{25a}$$

$$(\omega_0-\omega_s)^2\gg\delta^2. \tag{25b}$$

So within these conditions, expression (24) can be written as

$$I(\omega_0)=\beta F(\omega_0). \tag{26}$$

This expression shows that the inhomogeneous line shape $F(\omega)$ can be obtained from the intensities of the Fourier transform $I(\omega_0)$ of the echoes. In those cases where β depends on ω, care must be taken in using Eq. (26). Condition (25a) assures that the method will reproduce any feature in $F(\omega)$ with more width than the homogeneous broadening. On the other hand, condition (25b) imposes a limit to how close the reconstruction can be performed near a singularity. Again, the limitation of the reconstruction method depends on the homogeneous broadening.

B. Experimental details

BCPS samples were packed in a glass cylinder of 1 cm diameter and 2 cm length. The compound was provided by Fluka (Purum Grade) and was purified by zone melting. Additional measurements were carried out on a sample from Aldrich Chemical Company, Inc. (purity 97+%), but the same results were obtained. Measurements of the ^{35}Cl NQR line shape were performed from liquid-nitrogen temperature to 140 K. The NQR spectrometer has been described elsewhere.[4] The spectra were obtained by quadrature detection. The pulse sequence $(\pi/2)_0$-τ-$(\pi)_0$ was used in order to generate an echo signal, with a value $\tau=200$ μs. The $\pi/2$ pulse had 23 μs width and 150 W power. In order to assure that the reconstruction of $F(\omega)$ can be done using Eq. (26), the decay time of the echo signal was measured at different frequencies on the IC phase spectrum. The spectrometer temperature control provides temperature stability of the sample better than 0.1 K during the measurements.

IV. RESULTS

Prior to the measurements of the NQR line shape, the characteristic decay time T_D of the echo signal was measured at the edge peaks and in the middle of the NQR spectrum in the IC phase at 140 K. The measured decay time was $T_D=(700\pm30)$ μs for the three frequencies, being indistinguishable with the measured value at room temperature. After these results and according to Eq. (26), the inhomogeneous line shape $F(\omega)$ is proportional to $I(\omega)$. So, the inhomogeneous line shape can be reconstructed point by point. The ^{35}Cl NQR signals were recorded as a function of the irradiation frequency with 500 Hz minimum step. The experimental data were processed according to both methods discussed in Sec. III. Figures 3 and 4 shows the obtained profiles for $S_I(0;\omega)$ and $I(\omega)$, respectively. As can be clearly observed from Fig. 3, $S_I(0;\omega)$ is strongly smoothed with respect to $I(\omega)$. From the inspection of Figs. 3 and 4, the deviations between $S_I(0;\omega)$ and $I(\omega)$ involve the position, relative intensities (peak-peak, peak-valley), and widths of the observed peaks. Also, the sharpness of the spectral borders are quite different. The edges of the reconstructed spectra shown in Fig. 4 exhibit the typical abrupt profile associated with the IC phases of NQR spectra.[6] On the other hand, the spectra reported in Refs. 8, 9 seem to be affected by the same kind of distortion shown in Fig. 3. These distortions are more pronounced for temperatures near T_I, where the frequency separation between edge peaks is of the order of t_w^{-1}. In these cases, any fine structure of the spectral density, as the three peaks shown at 140 K in Fig. 4, is lost and

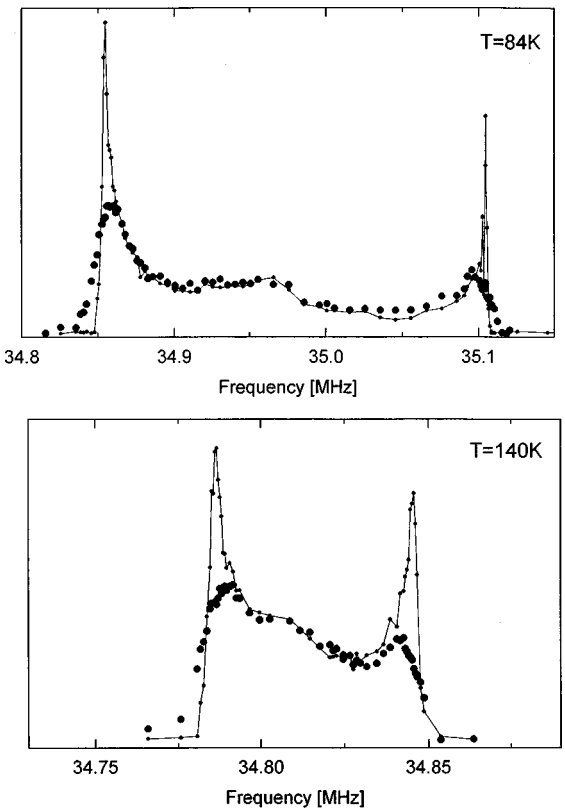

FIG. 3. Maximum amplitudes of the echo signals $S_I(0;\omega_0)$ generated by the sequence $\pi/2$-200 μs-π, as a function of the irradiation frequency ω_0, obtained at two temperatures in the incommensurate phase of BCPS. Circles indicate echo amplitudes. Points and solid line indicate Fourier-transform amplitudes of the same echoes, evaluated at ω_0. The profile of the echo intensities shows a considerable smoothing of the edge peaks with respect to the profile of Fourier-transform intensities.

a bell-shaped spectrum is obtained.[6,10] Our subsequent analysis of the NQR spectrum will be done using the data obtained through Fourier transform.

In addition to the sharp and intense edge peaks previously studied,[4] Fig. 4 shows a third weak peak that can be resolved in the intermediate frequency range. Figure 5 shows the temperature behavior of the NQR frequencies of the peaks. The structure of peaks in the NQR spectrum can be easily observed from 1 K below T_I. So, there is no evidence of fluctuations in the IC wave smearing out the fine structure of the NQR spectrum in the range of 10 K below T_I, as it was reported in Ref. 6. The smoothing of the NQR spectra near T_I observed in Ref. 6 is purely due to limitations of the experimental method chosen by these authors.

The plane-wave ''local'' model, with a linear relation between ν and the IC displacements, predicts a symmetric spectrum with only two edge peaks associated with maximum distortions. Therefore, this model cannot explain the observed NQR spectra of BCPS.

According to the results of Sec. II A, the addition of a quadratic term in expansion (1) could explain the presence of a third peak in the NQR spectrum. Nevertheless, as can be seen in Fig. 4, the central peak is clearly weaker than the others in all the temperature range. This fact is not in agreement with the intensity relationships (8) and (9) predicted by

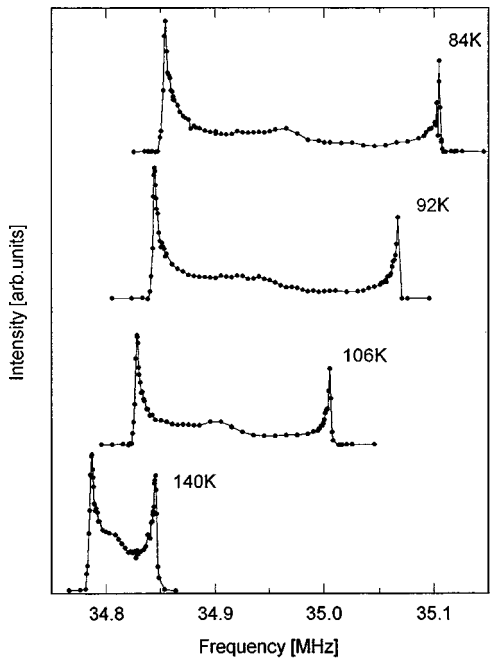

FIG. 4. Some ^{35}Cl NQR spectra of BCPS below T_I. These spectra were obtained from the Fourier transform of the echo signal as a function of the irradiation frequency, using the pulse sequence $\pi/2$-200 μs-π.

the plane-wave ''local'' model with linear and quadratic terms, where the intensity of the central peak assumes an intermediate value with respect to the edge peaks. So, this model cannot be applied to the IC phase of BCPS.

The temperature behavior of the coefficients ν_0, $|\nu_1|$, and ν_2 can be used as an additional test of the ''local'' model. By using Eq. (5) and the measured frequencies, $|\nu_1|$ and ν_2 were calculated as a function of temperature. Regarding that there are three peaks in the NQR spectrum, the necessary condition $|\nu_2|>|\nu_1|$ was imposed in order to discard one of the roots in Eq. (5a). Also, the two possible assignations $\nu_C \rightarrow \nu_{\text{Low Frec}}$ and $\nu_C \rightarrow \nu_{\text{High Frec}}$ were considered, according to Eqs. (7a) and (7b). The results obtained for $|\nu_1|$ and ν_2 were plotted in Fig. 6 for each valid assignation of ν_C. Also, the differences between the measured ν_C and the calculated ν_0 were plotted as a function of temperature in Figs. 7(a) and 7(b). The results are clearly in disagreement with the ''local'' model, which through expression (4) predicts a temperature-independent behavior of $\nu_C - \nu_0$. This behavior indicates that the possible assignations between measured and calculated frequencies are not compatible with expression (2), which sets the relation of the coefficients ν_n with

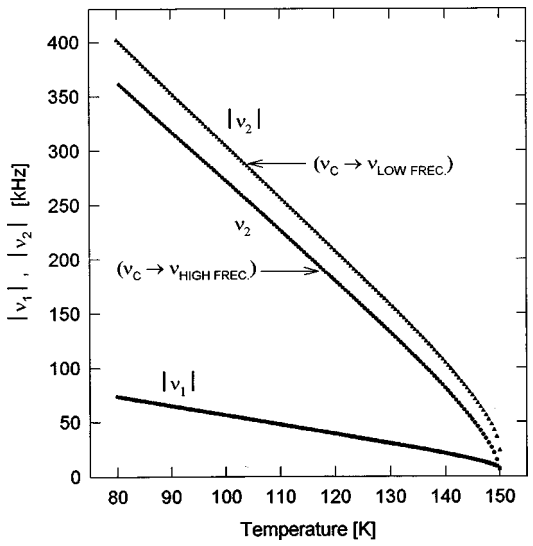

FIG. 6. Temperature behavior of the linear and quadratic coefficients ν_1 and ν_2 of the ''local'' model obtained from the measured frequencies, for the two possible assignations of the singularity ν_C with observed peaks.

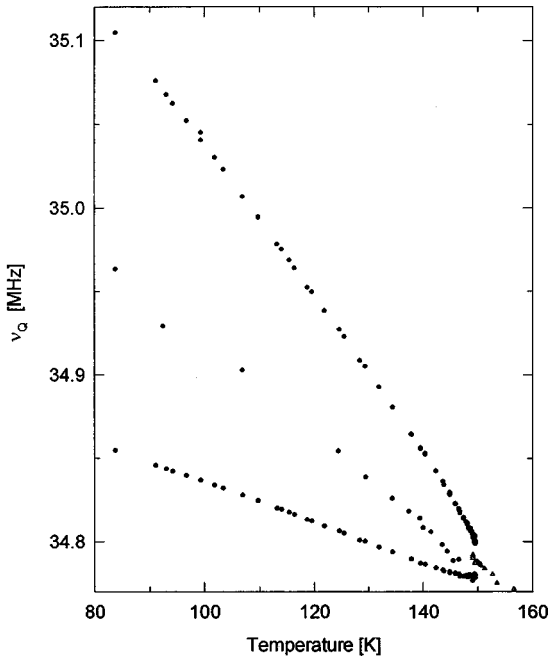

FIG. 5. Temperature behavior of the frequencies of the resolved NQR peaks in the incommensurate phase of BCPS.

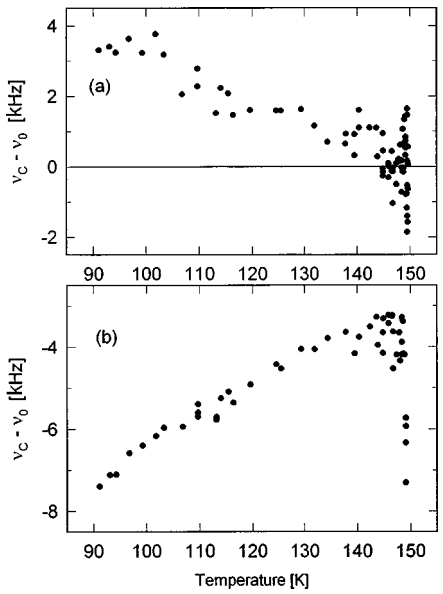

FIG. 7. Temperature behavior of the difference $\nu_c - \nu_0$ obtained from the measured frequencies, for the two possible assignations of the singularity ν_c with observed peaks. (a) $\nu_c \rightarrow \nu_{\text{High Frec}}$. (b) $\nu_c \rightarrow \nu_{\text{Low Frec}}$.

the order parameter of the phase transition.

By considering the results discussed above, it can be concluded that the plane-wave ''local'' model is not applicable to describe the NQR spectrum of BCPS in the IC phase.

The experimental results can be interpreted in terms of the general expansion summarized in Sec. II B. In this way, the simulation of the NQR spectrum in the IC phase was attempted, taking into account the simplified linear expression (15) for the EFG components. The first approximation was done by neglecting the asymmetry parameter in the expression of the NQR frequency. So, using Eq. (18), the spectral density was obtained from Eq. (20):

$$F(\nu) \propto \sum_{v'} \frac{1}{|[\sin v + 2r \sin(2v+\alpha)]_{v=v'}|}, \tag{27}$$

where $r \equiv \nu_2/\nu_1$. The NQR spectrum was calculated by evaluating numerically the convolution of $F(v)$ with a Lorentzian function of width $\delta = 450$ Hz. That value was obtained from the measurements of the spin-spin relaxation time T_2 using the relationship $\delta = 1/(\pi T_2)$. Figure 8(a) shows the best results obtained in the simulation of the spectrum at 84 K. A third peak and a slight asymmetry are introduced in the NQR spectrum, but the heights, widths, and the position of the third peak cannot be simultaneously fitted.

The natural improvement of the approximation is to retain the asymmetry parameter, by using expression (19) for the NQR frequency. Harmonics of order three and four are now expected in the modulation function of $\nu(v)$. Nevertheless, due to the great number of parameters involved, initially only one term was added to Eq. (15). So, a three harmonics modulation function for $\nu(v)$ was tentatively proposed:

$$\nu(v) = \nu_N + \nu_0 + 2\nu_1 \cos(v) + 2\nu_2 \cos(2v+\alpha) + 2\nu_3 \cos(3v+\beta), \tag{28}$$

and the spectral density associated with this function was

$$F(\nu) \propto \sum_{v'} \frac{1}{|[\sin v + 2r \sin(2v+\alpha) + 3p \sin(3v+\beta)]_{v=v'}|}, \tag{29}$$

with $p \equiv \nu_3/\nu_1$. The resulting spectrum is shown in Fig. 8(b). The features of the experimentally observed BCPS spectrum are quite well reproduced, including the heights of the three peaks. The result of adding only one-fourth harmonic to Eq. (28) was not satisfactory, because the asymmetry of the heights could not be reproduced. Also, the simulation including simultaneously harmonics of order three and four, gives not significant improvements with respect to the use of expression (28), probably due to limitations in the numerical implementation.

Table I shows the parameters r, p, α, and β obtained from the simulations of the NQR spectra at different temperatures. A good correlation of the values is observed as a function of temperature. The spectra at 140 K can be qualitatively reproduced with harmonics up to second order, but a better agreement is obtained with a little amplitude for the third harmonic, as can be seen in Fig. 9.

Unfortunately, the lack of knowledge concerning the numeric values of the gradients Φ^{Cl}_{1ij} and Φ^{C}_{1ij} in Eq. (14) precludes the comparison of the obtained quantities in Table I with the parameters of the atomic modulation functions. Nevertheless, it is encouraging that the relative weight of the second harmonic with respect to the fundamental in the *spatial* displacements measured by x-ray diffraction,[9] is the same order of magnitude as the coefficient r.

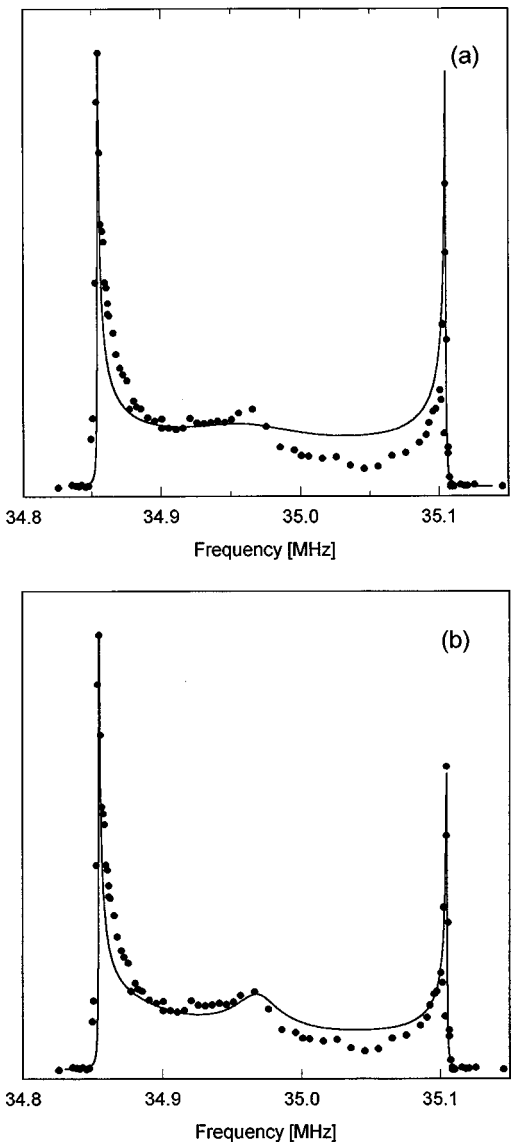

FIG. 8. Simulations of the NQR spectrum at 84 K. (a) Spectral density from expression (27). (b) Spectral density from expression (29), where modulation of the asymmetry parameter is considered.

TABLE I. The best set of parameters r, p, α, and β obtained from the simulation of the NQR spectra of BCPS at different temperatures [see expression (27) and (29) in text].

T (K)	r	p	α	β
84	0.2	0.11	−1.05	−0.78
92.4	0.2	0.09	−0.9	−0.5
106	0.2	0.10	−0.8	−0.8
140	0.2	0.02	−1.1	−0.1
140 (only second harmonic)	0.2		−1.16	

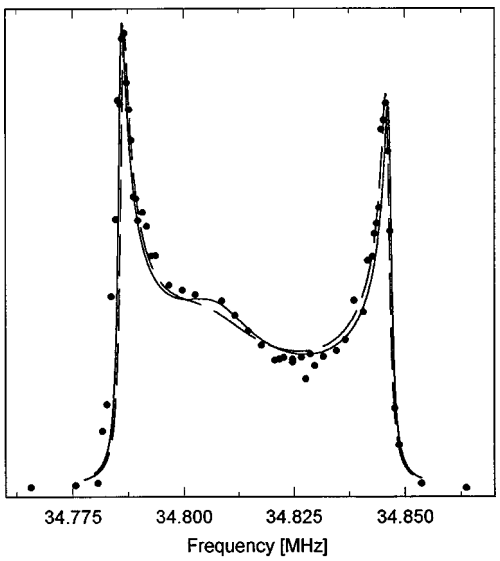

FIG. 9. Simulation of the spectrum at 140 K. Solid line indicates Spectral density from expression (27). Dashed line indicates spectral density from expression (29).

V. CONCLUSION

In this work, ^{35}Cl NQR data about the IC phase of BCPS were reported. The whole NQR spectrum was reconstructed using the Fourier transform of the nuclear signal. Two alternative approaches to handle the echo signal were discussed. It was remarked that recording the nuclear signal intensities $S_I(0;\omega_0)$ at different irradiation frequencies gives not, in general, the profile of the spectral density $F(\omega)$. This procedure implies a filtering of $F(\omega)$, causing the smoothing of abrupt variations of $F(\omega)$. On the other hand, the Fourier transform $I(\omega)$ of $S_I(t;\omega)$, evaluated at the irradiation frequency ω_0, gives the closest approximation to $F(\omega)$. The experimental results indicate the convenience of using the Fourier transform to reconstruct the spectral density, unless a flat line shape is expected.

Using these reliable data as a starting point, the features of the observed NQR spectra can be easily interpreted within the framework of the theoretical approach proposed by Perez-Mato, Walisch, and Petersson.[11] By using this formalism, it was possible to include explicitly the effects of the IC modulation on the asymmetry parameter, in the NQR frequency expansion in the IC phase. So, the main characteristics of the NQR spectrum of BCPS were well reproduced by assuming a non-negligible modulation of the asymmetry parameter and considering the atomic displacements $\mathbf{u}^\mu$ as two-harmonic functions, according to the available information from x-ray diffraction and neutron scattering. Also, the experimental results exclude the possibility of strong fluctuations of the IC wave smearing out the NQR spectrum, because the three peaks can be clearly resolved from 80 to 149 K.

On the other hand, the cumbersome problem of correlating the NQR frequency distribution with the atomic displacements $\mathbf{u}^\mu$ in an IC phase, was clearly revealed through expressions (11) and (19). To obtain information about the $\mathbf{u}^\mu$ through the analysis of the pure ^{35}Cl NQR spectrum, it is necessary to know all the relevant derivatives Φ^μ_{nij} for each EFG tensor element V_{ij}. Even in the simplified expression (14), this fact implies the knowledge of six parameters for each element V_{ij}. Taking into account expression (19) when $\eta \neq 0$, the NQR frequency depends at least on two elements of the EFG tensor, so 12 parameters are required.

Finally, some general predictions of the plane-wave ''local'' model have been pointed out. The relative peak intensities and the temperature dependence of the coefficients ν_n were calculated for the case of linear and quadratic terms in the relation between the NQR frequency and the order parameter. These results provide a useful tool to test the applicability of model in a particular case, by rapid inspection of the relative intensities of the NQR peaks. For the BCPS, it was readily concluded that the ''local'' model is not applicable at any temperature below T_I.

ACKNOWLEDGMENT

The authors thank CONICET for financial support.

[1] R. Blinc, Phys. Rep. **79**, 343 (1981); **79**, 395 (1981).
[2] D. Pusiol, A. Wolfenson, and A. Brunetti, Phys. Rev. B **40**, 2523 (1989).
[3] J. Etrillard, B. Toudic, M. Bertault, J. Even, M. Gourdji, A. Péneau, and L. Guibé, J. Phys. I **3**, 12 (1993).
[4] J. Schneider, A. Wolfenson, and A. Brunetti, J. Phys.: Condens. Matter **6**, 11 035 (1994).
[5] R. Blinc, T. Apih, J. Dolinšek, U. Mikac, D. C. Ailion, and P. H. Chan, Phys. Rev. B **51**, 1354 (1995).
[6] U. Mikac, T. Apih, M. Koren, J. Dolinšek, J. Seliger, J. Slak, and R. Blinc, Phys. Rev. B **54**, 9141 (1996).
[7] R. Blinc, J. Seliger, and S. Zumer, J. Phys. C **19**, 2613 (1986).
[8] The differentiation between the so-called ''local'' and nonlocal model is not strictly valid, as it was pointed out in Ref. 11, so the word *''local''* will be used between quotes.
[9] F. Zúñiga, J. Perez-Mato, and T. Breczewski, Acta Crystallogr., Sect. B: Struct. Sci. **49**, 1060 (1993).
[10] J. Etrillard, J. Even, M. Sougoti, S. Launois, S. Longeville, and B. Toudic, Solid State Commun. **87**, 47 (1993).
[11] J. M. Perez-Mato, R. Walisch, and J. Petersson, Phys. Rev. B **35**, 6529 (1987).
[12] M. Rubinstein and P. Taylor, Phys. Rev. B **9**, 4258 (1974).
[13] G. Jellison, G. Petersen, and P. Taylor, Phys. Rev. B **22**, 3903 (1980).
[14] P. Katowski and M. Mackowiak, Appl. Magn. Reson. **9**, 409 (1995).
[15] J. C. Pratt, Mol. Phys. **34**, 539 (1977).
[16] S. Su and R. Armstrong, J. Magn. Reson., Ser. A **101**, 265 (1993).
[17] Y. Y. Tong, J. Magn. Reson., Ser. A **119**, 22 (1996).